PERGAMON

International Journal of Multiphase Flow 26 (2000) 327–337

International Journal of Multiphase Flow

www.elsevier.com/locate/ijmulflow

Brief Communication

Numerical calculation of turbulent stratified gas–liquid pipe flows

Charles H. Newton, Masud Behnia*

School of Mechanical and Manufacturing Engineering, University of New South Wales, Sydney, 2052, Australia

Received 24 March 1998; received in revised form 19 January 1999

1. Introduction

The prediction of pressure loss and void fraction in gas–liquid pipe flows has been of considerable research interest since the 1930s. Application may be found in a wide variety of areas including the petroleum and chemical processing industries, in steam generation and refrigeration equipment, and in nuclear reactors. Past approaches to such calculations have been mainly empirical, and literally dozens of data correlations for the respective design parameters appear in the literature. Unfortunately, most of these correlations were developed under laboratory conditions, and are inaccurate when scaled-up to oilfield applications (Gregory and Fogarasi, 1985; Simpson et al., 1987), gas-condensate systems (Battara et al., 1985), and steam-water systems (Idsinga et al., 1977). Further, their predictive capabilities are generally biased towards the flow conditions on which they are based (Mandhane et al., 1977).

More recent approaches to the problem have resulted in the development of so-called 'mechanistic' models, which allow analysis of specific flow patterns based primarily on their physical geometry. In horizontal flow, where gravitational separation of the phases is common, the most notable of these are due to Taitel and Dukler (1976) for stratified flow, and Dukler and Hubbard (1975) for slug flow. It is noted however, that for stratified flow models, the number of empirical inputs required (i.e. the shear stresses) exceeds the number of derived outputs (i.e. the pressure gradient and liquid holdup) by one. Slug flow models generally require further input variables, such as slug translational velocity, frequency and holdup. Thus, mechanistic approaches may actually lead to an increase in the requirement of empirical information.

* Corresponding author.

PII: S0301-9322(99)00010-5

The use of Computational Fluid Dynamics (CFD) techniques for the calculation of pressure drop and void fraction in gas–liquid pipe flow is not common. Previous work has been mainly restricted to the use of Marker and Cell or Volume of Fluid (VOF) methods for two- and three-dimensional problems in free surface motion and bubble growth. However, for stratified flows some investigators have attempted to use separated flow models, obtaining steady flow solutions with the interface treated as a free-surface type boundary condition. Such investigations in rectangular ducts include those of Akai *et al.* (1981), Issa (1988) and Srichai *et al.* (1995).

One of the early CFD models of turbulent stratified flow in a horizontal pipe was presented by Shoham and Taitel (1984). The gas region was treated as a bulk flow and the liquid region flow field was calculated using a finite difference solution of the two-dimensional axial momentum equation, with the turbulent viscosity calculated from a zero equation model. Solutions for turbulent liquid flows were obtained in horizontal and slightly inclined pipes of 25.4 mm diameter. However, the published form of the axial momentum equation used in this study did not include first order viscosity gradient terms, casting some doubt over the validity of the results.

Issa (1988) also obtained solutions for stratified gas–liquid pipe flow with a smooth interface. The flow field in both phases was calculated using the standard k–ε turbulence model with wall functions. The results showed reasonable agreement with predictions from the mechanistic model of Taitel and Dukler (1976), however, they were confined to a relatively small pipe diameter of 25.4 mm.

The primary purpose of the present work is to extend the approach of Issa (1988), to allow predictions of pressure gradient and liquid holdup for turbulent, smooth-stratified two-phase flow in a larger, 50 mm diameter, pipe. The two-dimensional axial momentum equations are solved in each phase, and the turbulent viscosity is obtained with a low Reynolds number k–ε model, which allows resolution of the flow in the viscous sub-layer in the vicinity of the wall and gas–liquid interface. The only empirical information required in our approach is the specification of damping functions in the turbulence model.

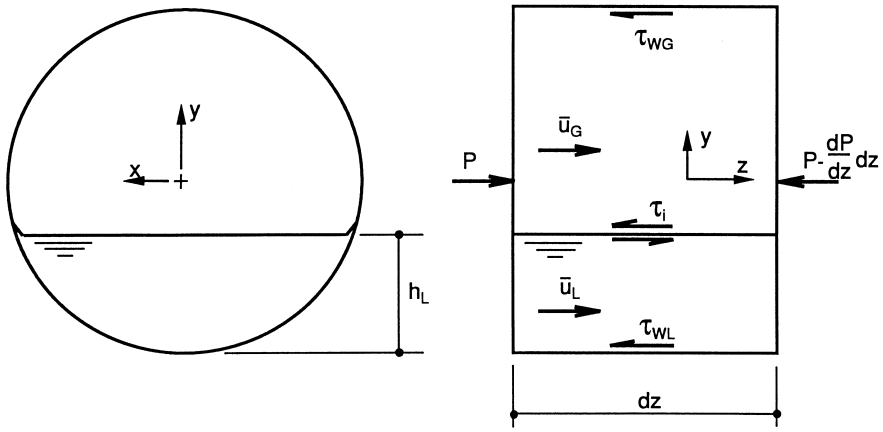

Fig. 1. Schematic representation of stratified-smooth gas–liquid pipe flow.

The calculation of the two-phase flow by such means offers distinct advantages over other, more commonly used, methods. By directly calculating flow near the boundaries of each phase, we are able to directly predict the spatial wall and interfacial shear-stress distributions, in order to assess the viability of commonly used empirical relations. Further, calculation of the two-dimensional velocity field allows estimation of the momentum correction factor for each phase, which would be useful where liquid height gradients or variable gas densities exist. Such calculations have not previously appeared in the literature.

2. Calculation procedure

Consider incompressible stratified gas–liquid flow in a horizontal pipe, as shown in Fig. 1. For brevity, the present results are restricted to flows in which the gas–liquid interface is smooth. Under steady-flow conditions, the axial pressure gradient $\mathrm{d}P/\mathrm{d}z$ is balanced by the liquid and gas wall shear stresses, denoted by τ_{WL} and τ_{WG}, respectively. Under such circumstances, assuming a uni-directional flow in both phases, except for the fluctuating components in the cross-stream directions, the axial momentum equation is given by:

$$\frac{dP}{\mathrm{d}z} = \mu\left[\frac{\partial^2 w}{\partial x^2} + \frac{\partial^2 w}{\partial y^2}\right] + \frac{\partial}{\partial x}(-\rho\overline{u'w'}) + \frac{\partial}{\partial y}(-\rho\overline{v'w'}) \tag{1}$$

where u, v and w are the velocities in the cross-stream, vertical, and axial directions, respectively, and the prime denotes a fluctuating quantity. Assuming isotropic turbulence, the Reynolds stresses in Eq. (1) are given by the usual definition of turbulent viscosity, i.e. $-\rho\overline{u'w'} = \mu_{\mathrm{t}}(\partial u/\partial z + \partial w/\partial x)$, $-\rho\overline{v'w'} = \mu_{\mathrm{t}}(\partial v/\partial z + \partial w/\partial y)$. Since, for unidirectional flow, $\partial u/\partial z = \partial v/\partial z = 0$, then Eq. (1) can be rearranged to give:

$$\frac{\mathrm{d}P}{\mathrm{d}z} = \mu_{\mathrm{e}}\left[\frac{\partial^2 w}{\partial x^2} + \frac{\partial^2 w}{\partial y^2}\right] + \frac{\partial \mu_{\mathrm{t}}}{\partial x}\frac{\partial w}{\partial x} + \frac{\partial \mu_{\mathrm{t}}}{\partial y}\frac{\partial w}{\partial y}, \tag{2}$$

where $\mu_{\mathrm{e}} = \mu + \mu_{\mathrm{t}}$ is the effective viscosity.

In order to eliminate the use of wall functions, the turbulent viscosity is calculated here using a low Reynolds number k–ε model. For the present system this is given by:

$$\mu_{\mathrm{t}} = f_\mu C_\mu \rho k^2/\varepsilon,$$

$$\Gamma_k\left[\frac{\partial^2 k}{\partial x^2} + \frac{\partial^2 k}{\partial y^2}\right] + \frac{1}{\sigma_{\mathrm{k}}}\left[\frac{\partial \mu_{\mathrm{t}}}{\partial x}\frac{\partial k}{\partial x} + \frac{\partial \mu_{\mathrm{t}}}{\partial y}\frac{\partial k}{\partial y}\right] + \mu_{\mathrm{t}}\left[\left(\frac{\partial w}{\partial x}\right)^2 + \left(\frac{\partial w}{\partial y}\right)^2\right] - \rho\varepsilon = 0,$$

$$\Gamma_{\mathrm{e}}\left[\frac{\partial^2 \varepsilon}{\partial x^2} + \frac{\partial^2 \varepsilon}{\partial y^2}\right] + \frac{1}{\sigma_\varepsilon}\left[\frac{\partial \mu_{\mathrm{t}}}{\partial x}\frac{\partial \varepsilon}{\partial x} + \frac{\partial \mu_{\mathrm{t}}}{\partial y}\frac{\partial \varepsilon}{\partial y}\right] + C_1 f_1 \frac{\varepsilon}{k}\mu_{\mathrm{t}}\left[\left(\frac{\partial w}{\partial x}\right)^2 + \left(\frac{\partial w}{\partial y}\right)^2\right] - C_2 f_2 \rho\frac{\varepsilon^2}{k} = 0, \tag{3}$$

where $\Gamma_k = (\mu + \mu_{\mathrm{t}}/\sigma_k)/\rho$, $\Gamma_\varepsilon = (\mu + \mu_{\mathrm{t}}/\sigma_\varepsilon)/\rho$, with $\sigma_k = 1.0$, $\sigma_\varepsilon = 1.3$, $C_\mu = 0.09$, $C_1 = 1.92$ and

$C_2 = 1.3$. Closure of the model is thus achieved by prescribing the wall damping functions f_μ, f_1, and f_2. An evaluation of several formulations of these parameters has been performed by Patel et al. (1985). In their study the equations due to Lam and Bremhorst (1981) showed good agreement with experimental data obtained in turbulent pipe flow, and have been adopted here. These are given by:

$$f_\mu = [1 - \mathrm{e}^{-0.0165R_k}]^2\left(1 + \frac{\beta}{R_\mathrm{T}}\right), \quad f_1 = 1 + \left(\frac{0.05}{f_\mu}\right)^3, \quad f_2 = 1 - \mathrm{e}^{-R_\mathrm{T}^2}, \tag{4}$$

where $R_k = \rho\sqrt{k}d_\mathrm{w}/\mu$ and $R_\mathrm{T} = \rho\mathrm{k}^2/\mu\varepsilon$. Lam and Bremhorst (1981) used $\beta = 20.5$ for single-phase pipe flow, where the characteristic distance d_w is defined as the radial distance to the nearest wall. However, the presence of the interface in stratified gas–liquid flow also acts to dampen turbulence, and in the present work d_w is taken as the distance to the nearest surface i.e. either the wall or interface, as recommended by Demuren and Rodi (1984). For the present co-ordinate system, this distance is the smaller of:

$$\eta = \frac{D}{2} - \sqrt{x^2 + \left[y - \left(\frac{D}{2} - h_\mathrm{L}\right)\right]^2}, \quad \eta = \mid y \mid, \tag{5}$$

where η is normal to the respective surface, D is the pipe diameter, and h_L is the mean liquid height.

Results obtained for single-phase gas flows in non-circular ducts (Newton, 1997), suggested that β may be flow regime dependent. Consideration of Eq. (4) indicates that as the transition to laminar flow is approached, it may be expected that $\beta/R_\mathrm{T}^2 \to -1$ to mimic the destruction of the turbulent viscosity. Further, it is reasonable to assume that $\beta \to 20.5$ at relatively high Reynolds numbers (i.e. $Re_\mathrm{G} \approx 50{,}000$), in accordance with the findings of Lam and Bremhorst (1981). Thus, on the basis of additional numerical experimentation, the following expression was adopted in all the calculations:

$$\beta = 20.5[1 - 1.45\ \exp(-1.4 \times 10^{-4} Re_\mathrm{G})]. \tag{6}$$

The assumption of isotropic turbulence is not made without restrictions. Both Nallasamy (1987) and Rodi (1993) observe that since the k–ε model assumes an isotropic eddy viscosity, it has no in-built mechanism for the development of secondary flows, which may be caused by non-zero differences in the Reynolds stresses in planes normal to the axial direction for flow in non-circular ducts. Such an occurrence may become significant in stratified gas–liquid flow as the height of the interface approaches the centre of the pipe. Demuren and Rodi (1984) and Edwards and Jensen (1993) have observed that the presence of this motion has a noticeable effect on the local wall shear stress. However, the calculation of secondary flow requires the independent evaluation of all the Reynolds stresses, involving a significant increase in computational cost for what is likely to be a marginal increase in predictive capability.

The final elements of the model are the boundary conditions at the wall and interface. For the solid walls the following boundary conditions are used:

$$w = k = \mu_\mathrm{t} = 0 \tag{7}$$

Since μ is constant, then $\mu_e = \mu$ at the walls. The boundary condition for the dissipation is usually found by applying $\partial k/\partial \eta = \mu_t = 0$ to the transport equation for k. The result is:

$$\varepsilon_w = \frac{\mu}{\rho}\left(\frac{\partial^2 k}{\partial \eta^2}\right)_w. \tag{8}$$

However, as Eq. (8) involves the solution of the turbulent kinetic energy field, a more numerically convenient form of the wall boundary condition has been successfully applied by Patel et al. (1985), and is given by:

$$\frac{\partial \varepsilon_w}{\partial \eta} = 0. \tag{9}$$

Hanjalic and Launder (1976) have used Eq. (9) as a boundary condition for the dissipation in their Reynolds stress model, and it is used for all wall boundaries in the present numerical calculations.

It might be expected that the boundary conditions for coupling of the phases at the interface are somewhat less straightforward than those for a solid wall. However, Nezu and Nakagawa (1993) have suggested that the presence of a free surface acts to reduce the length scale of turbulence, in a similar manner to the presence of a wall. Rodi (1993) has proposed that the presence of a free surface can, as a first approximation, be treated as a moving wall. In the calculations for smooth-stratified flow presented here, this approximation is adopted. Hence, the following conditions are used at the free surface:

$$w_L = w_G, \quad k_L = k_G = 0, \quad \mu_{t_G} = \mu_{t_L} = 0, \tag{10}$$

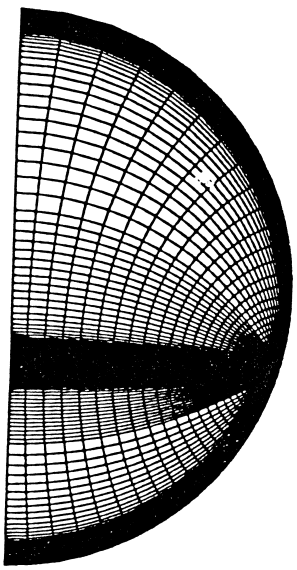

Fig. 2. Distribution of grid points in the physical domain. Adapted mesh for $j_L = 0.03$ m/s, $j_G = 1.67$ m/s, and $h_L = 13.68$ mm.

with the dissipation calculated using Eq. (9). Thus, the interface acts as a moving wall with the two phases coupled through the velocity field. The numerical solution of the flow equations is conducted separately for each phase, with these boundary conditions providing the coupling between these phases. The liquid height h_L (and consequently, the computational grid) is continually adjusted during the calculations to satisfy continuity requirements. For the gas region calculations the velocity boundary condition at the interface is obtained from the solution of the liquid-flow field, except at the first height iteration where the velocity profile across the interface is introduced empirically as a starting condition for more rapid convergence. The interfacial shear stresses resulting from the calculated gas-flow field are then used to provide a boundary condition for the liquid region, by assuming:

$$\tau_{i_G} = \tau_{i_L} \tag{11}$$

across the interface. To compensate for the turbulence damping effect of the interface, the wall functions given by Eq. (4) are used on both sides of the free surface.

The model Eqs. (1)–(11) were transformed into the bipolar coordinate system for adaptation to the present geometry. Such a transformation is given elsewhere (e.g. Issa, 1988) and is not repeated here. An example of a typical physical grid mapped in the bipolar coordinate system is given in Fig. 2. Note the compactness of the grid in the near wall and interfacial regions. Adequate resolution of large gradients of k and ε in the viscous sub-layers of these regions suggests a nominal grid spacing of $\eta^+ = \eta\sqrt{\rho\tau_w}/\mu \approx 1$, where τ_w is the local wall shear stress. In the present calculations 40 grid points were placed approximately in the region $0 < \eta^+ < 40$ at all boundaries. More comprehensive details of the grid construction can be found in Newton (1997).

The governing flow equations were solved in each phase using an iterative finite difference technique. Both first- and second-order differencing schemes were used, but due to the close grid spacing, little difference was observed in the results. The input variables are pipe diameter D, and liquid and gas superficial velocities j_L and j_G. The model predicted the axial pressure gradient and liquid holdup, and gave the two-dimensional velocity and turbulence fields. A post-processor was used to derive the wall and interfacial shear stress distributions from the calculated results. Computations were performed on both an HP-9000 workstation, and a Pentium PC.

3. Results and discussion

In the present model it is assumed that the mean flow in both phases is uni-directional, steady, and fully developed. Under such circumstances there can be no interface level gradient unless there is a change in gas density, which may be due either to the favourable pressure gradient, or to heat transfer through the pipe walls. For the stratified flow conditions modelled here, the pressure gradients are small and the fluid properties are assumed to be those at atmospheric temperature and pressure. It is also noted that at small liquid holdups interface may contain significant curvature in the cross-stream direction. Under such circumstances the present interfacial boundary conditions can not be expected to accurately simulate the flow. The calculations shown here are generally restricted to mean liquid holdups higher than 0.15.

Calculations of pressure gradient and liquid holdup are compared with the mechanistic model of Taitel and Dukler (1976), and the experimental data of Newton and Behnia (1996) in

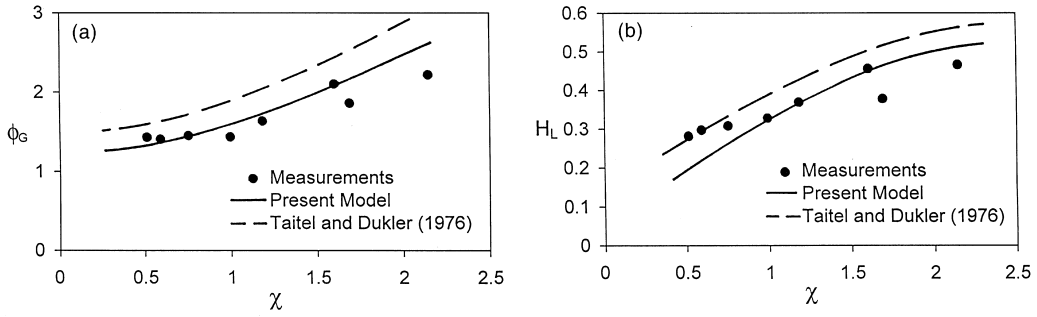

Fig. 3. Comparison of predicted and measured data for stratified-smooth flow: (a) axial pressure gradient, (b) liquid holdup.

Fig. 3. The lack of experimental data is due to the difficulty in obtaining pressure gradient measurements under the conditions required to maintain a smooth gas–liquid interface, i.e. low bulk velocities, in both phases. For this reason the pressure gradient measurements in particular incorporate a reasonably significant degree of uncertainty, estimated here to be as high as 30%, at the lowest flow rates.

The pressure gradient results are represented by a gas pressure gradient multiplier, defined as:

$$\phi_G = \sqrt{\frac{(dP/dz)_{TP}}{(dP/dz)_{GS}}}, \tag{12}$$

where the subscripts TP and GS denote two-phase and gas only. Both the pressure gradient and liquid hold-up results are correlated with the Lockhart–Martinelli parameter, defined by:

$$\chi = \sqrt{\frac{(dP/dz)_{LS}}{(dP/dz)_{GS}}}, \tag{13}$$

where the subscript LS denotes single phase liquid flow. The results indicate that the present model is quite successful at predicting both the pressure gradient and liquid holdup. It is noted that the smooth stratified flow results of Issa (1988), obtained in a pipe of diameter 25.4 mm, closely followed the predictions of the Taitel and Dukler (1976) model.

In order to check the sensitivity of the revised turbulence model, various constant values of β_G were used in the gas region, whilst holding β_L constant in the liquid region. The results, shown in Table 1, indicate that such a variation has little effect on the overall calculations. The

Table 1
Effect of β_G for $\beta_L = 3.0$, $j_L = 0.07$ m/s, $j_G = 0.93$ m/s

β_G	dP/dz (Pa/m)	h_L (mm)
15.0	2.0	13.6
9.0	2.0	13.7
4.0	1.9	13.9

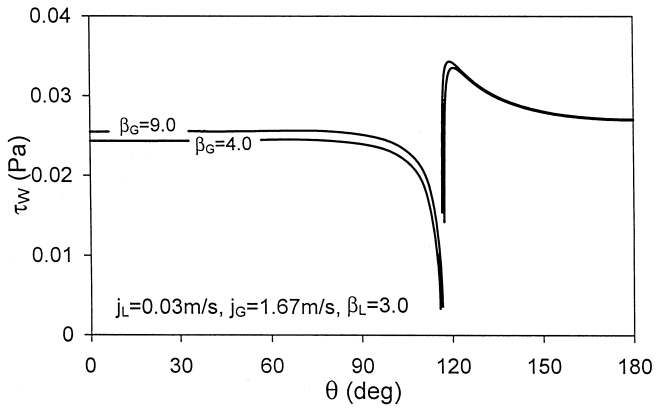

Fig. 4. Radial distribution of the wall shear stress. θ = zero at the top of the pipe.

variation in the wall shear stress profile, shown in Fig. 4, also shows that the effect of variable β is quite small. The relaxation of gas wall shear stress observed experimentally by Kowalski (1987), is also evident in Fig. 4. A significant rise in the liquid wall shear stress in the immediate vicinity of the interface is also evident, and was observed in all the computations reported here. Direct comparison with measurements is impossible at such low Reynolds numbers, where the Preston tubes used in the experiments became ineffective. This is also the case for velocity profile measurements using Pitot tubes.

A representative profile for the interfacial shear stress is shown as a function of variable gas region β in Fig. 5. It is noted that this parameter is essentially constant across the interface, except in the near wall region where a relaxation is observed.

The wall and interfacial shear stresses were averaged over their respective domains and average friction factors were then calculated from $f = 2\bar{\tau}/\rho\bar{u}^2$, where $\bar{\tau}$ is the perimeter-averaged shear stress, and $\bar{u}$ is the area-averaged phase velocity. Results for the gas wall region are shown in Fig. 6, where it may be observed that the Blasius equation increasingly over-predicts the calculated values as the phase Reynolds number is increased, as observed experimentally by Newton and Behnia (1996). The average predicted interfacial friction factors

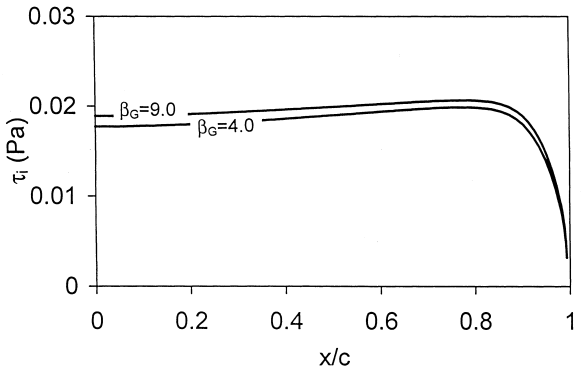

Fig. 5. Calculated distribution of the interfacial shear stress for $j_L = 0.03$ m/s, $j_G = 1.67$ m/s.

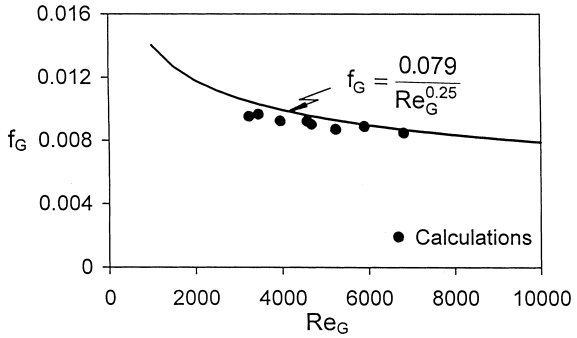

Fig. 6. Comparison of the calculated average gas wall friction factor calculations with the Blasius equation.

are compared with the gas wall friction factors in Fig. 7. It is commonly assumed (e.g. Taitel and Dukler, 1976; Sadatomi et al., 1993) that $f_i = f_G$, especially for smooth gas–liquid interfaces. The present calculations suggest that the gas wall shear stress is substantially higher than that at the interface. Finally, it is observed that the liquid wall friction factors are considerably over-predicted by the single phase Blasius type equation, as shown in Fig. 8. Under such circumstances the ratio of wall to cross-sectional area of the liquid region is far

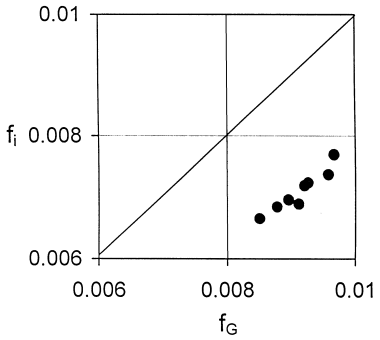

Fig. 7. Comparison of calculated average gas wall and interfacial friction factors.

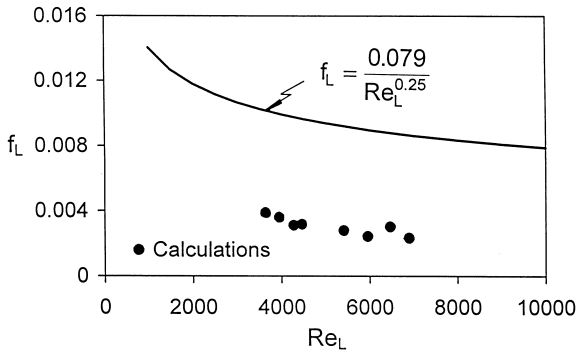

Fig. 8. Comparison of the calculated average liquid wall friction factors with the Blasius equation.

greater than for a fully circular region, and equations based on full pipe flow cannot be relied upon to give accurate results for friction factor. The calculated phase momentum correction factors also consistently differ from those expected from single-phase pipe flow. Over the range of calculations considered here the gas and liquid correction factors were both approximately 1.12, which are considerably higher than those expected in turbulent single-phase pipe flow.

4. Conclusion

Numerical calculations of axial pressure gradient, liquid holdup, and the flow and turbulence fields in a stratified gas–liquid pipe flow have been presented. A low Reynolds number k–ε formulation was used to model the turbulent viscosity. This model incorporated wall damping functions obtained from single-phase pipe flow. Although minor 'tuning' of the wall damping functions was performed, the results indicated that such tuning had little effect, and agreement with experimental data was excellent. Evidently, standard wall functions have sufficient generality to be applied to the two-phase flows considered here. This conclusion contrasts with the poor performance of commonly used single-phase flow relationships to model wall and interfacial shear stresses, as demonstrated by the present calculations. However, since the present model does not rely on such information, it is believed that it may have considerable value in further research into more general stratified two-phase flows.

References

Akai, M., Inoue, A., Aoki, S., 1981. The prediction of stratified two-phase flow with a two-equation model of turbulence. International Journal of Multiphase Flow 7, 21–39.

Battara, V., Mariani, O., Gentilini, M., Giachetta, G., 1985. Condensate line correlations for calculating holdup, friction compared to field data, Oil and Gas Journal 148–152.

Demuren, A.O., Rodi, W., 1984. Calculation of turbulence driven secondary motion in non-circular ducts. Journal of Fluid Mechanics 140, 180–222.

Dukler, A.E., Hubbard, M.G., 1975. A model for gas–liquid slug flow in horizontal and near horizontal tubes. Industrial Engineering and Chemistry Fundamentals 14, 337–347.

Edwards, D.P., Jensen, M.K., 1993. Calculation of turbulence-driven secondary flows—Part II: predictions for fully developed flow in a square duct. ASME Winter Annual Meeting, New Orleans, 93-WA/HT-31.

Gregory, G.A., Fogarasi, M., 1985. A critical evaluation of multiphase gas–liquid pipeline calculation methods. In: Proc. 2nd Intl. Conf. on Multiphase Flow, London, pp. 93–108.

Hanjalic, K., Launder, B.E., 1976. Contribution towards a Reynolds stress closure for low Reynolds number turbulence. Journal of Fluid Mechanics 74, 593–610.

Idsinga, W., Todreas, N., Bowring, R., 1977. An assessment of two-phase pressure drop correlations for steam water systems. International Journal of Multiphase Flow 3, 401–413.

Issa, R.I., 1988. Prediction of turbulent, stratified, two-phase flow in inclined pipes and channels. International Journal of Multiphase Flow 14, 141–154.

Kowalski, J.E., 1987. Wall and interfacial shear stress in stratified flow in a pipe. AIChE Journal 33, 274–281.

Lam, C.K.G., Bremhorst, K., 1981. A modified form of the k–ε model for predicting wall turbulence. ASME Journal of Fluids Engineering 103, 456–460.

Mandhane, J.M., Gregory, G.A., Aziz, K., 1977. Critical evaluation of friction pressure-drop prediction methods for gas–liquid flow in horizontal pipes. Journal of Petroleum Technology 29, 1348–1358.

Nallasamy, M., 1987. Turbulence models and their applications to the prediction of internal flows: A Review. Computers and Fluids 15, 151–194.

Newton, C.H., 1997. An experimental and numerical study of stratified gas–liquid flow in horizontal pipes. PhD Thesis, University of New South Wales.

Newton, C.H., Behnia, M., 1996. Estimation of wall shear stress in horizontal gas–liquid stratified flow. AIChE Journal 42, 2369–2373.

Nezu, I., Nakagawa, H., 1993. Turbulence in Open-Channel Flows. IAHR Monograph Series.

Patel, V.C., Rodi, W., Scheurer, G., 1985. Turbulence models for near-wall and low Reynolds number flows: A review. AIAA Journal 23, 1308–1319.

Rodi, W., 1993. Turbulence Models and Their Application in Hydraulics—A State of the Art Review. IAHR Monograph Series, 3rd ed.

Sadatomi, M., Kawaji, M., Lorencez, C.M., Chang, T., 1993. Prediction of liquid level distribution in horizontal gas–liquid stratified flows with interfacial level gradient. International Journal of Multiphase Flow 19, 987–997.

Shoham, O., Taitel, Y., 1984. Stratified turbulent-turbulent gas–liquid flow in horizontal and inclined pipes. AIChE Journal 30, 377–385.

Simpson, H.C., Rooney, D.H., Gilchrist, A., Grattan, E., Callender, T.M.S., 1987. An assessment of some two-phase pressure gradient, holdup, and flow pattern prediction methods in current use. In: Proc. 3rd Intl. Conf. on Multiphase Flow, The Hague, pp. 22–32.

Srichai, S., Jayanti, S., Hewitt, G.F., 1995. CFD Techniques for separated two-phase flows. First Asian CFD Conference, Hong Kong, 16–19 January, 1025–1031.

Taitel, Y., Dukler, A.E., 1976. A model for predicting flow regime transitions in horizontal and near horizontal gas–liquid flow. AIChE Journal 22, 47–55.